Radiation Hazards in Space

A statistical approach to doses in various body regions provides a realistic measure of the hazard.

David L. Dye and Maurice Wilkinson

Estimation of the radiation hazard to crew personnel in a space vehicle involves concepts drawn from such differing disciplines as solar, cosmic ray, and ionospheric physics; celestial mechanics; radiation shielding and dosimetry; radiation biology; genetics; and stress physiology. Generally, the problem of the radiation hazard in space has been divided, like Gaul, into three parts: the environment, the modification of that environment by structure and shielding, and the effects of the penetrating radiation on occupants of the vehicle. There is, of necessity, interplay between these facets of the problem; as long as this fact is realized, the compartmentation is a convenient one. In this article we gather together information from all three categories in order to clarify the nature of the hazard and to quantify the hazard on the basis of some reasonable assumptions. The treatment is not intended to be either exhaustive or erudite, but a few conclusions are drawn and some directions for further studies are indicated.

Specifically, our aim is to present the results of calculations of the amount of radiation from protons trapped in the earth's magnetic field or emitted in solar flares that is absorbed at various points in the body of a human being seated in a spherical-shell vehicle, the body tissues themselves being considered part of the shielding. A rather hypothetical dose value has been reported in most calculations of radiation dose in space (see, for example, *1–3*). This is the ionization dose in water immediately behind a "one-dimensional" (that is, spherically symmetric) shield. While this value is indicative of the radiation hazard to a man in space, the biologically significant doses are those actually absorbed in the vital or critically radiosensitive organs of the astronaut. In computing these doses one must consider the shielding provided by the human body itself as well as the structural shielding of the vehicle. This computation problem has been discussed elsewhere; here we present body-point doses calculated for more recently determined energy spectra than those on which the earlier results (*4*) were based, and with better data for the production of secondary particles than we had in the earlier studies.

Dr. Dye is chief of the Radiation Effects Laboratory of the Boeing Company, Seattle, Washington; Mr. Wilkinson is a research scientist in the Nuclear and Space Physics Unit of the Boeing Company.

Radiation Environment of Space

The parameters of interest in the radiation environment of space are (i) particle types, and (ii) fluxes—their variation with time and their distributions, in energy, in angle of incidence, and with position in space. Much research remains to be done to define these parameters completely, but enough data already exist to permit a realistic, if approximate, evaluation of the radiation hazard in space. Electrons trapped at high altitudes, both natural electrons and those from thermonuclear explosions, have been considered elsewhere. Here we consider only trapped protons, cosmic rays, and solar protons, dealing with the last category in some detail.

The belts of trapped natural protons and electrons that encircle the earth have been extensively probed by satellites. The lower fringes of the proton belt have been studied, also, by the use of nuclear emulsions and shielded counters in ballistic trajectories (*5*). The available data have permitted analysis in terms of geomagnetic trapping theory. The observed intensities of the trapped particles can be plotted by geomagnetic coordinates, and vehicle trajectories can be plotted by these same coordinates (*6*). Then a line integral obtained with respect to real time along a trajectory will yield a value for total particle flux incident on the vehicle (*7*). By means described elsewhere (*4*), the dose to specific body points may be obtained from this value.

It has generally been supposed that the low rates for ionization dose from the primary cosmic rays imply that this part of the radiation environment of space presents no hazard. However, H. J. Schaefer has pointed out that, although the total ionization (the dose) is low, the ionization density (or linear energy transfer) is high for these heavy particles (*8*). Hence, their biological effects may be out of proportion to their dose contribution. The flux and energy spectra of the protons, of helium nuclei, and of heavier nuclei in cosmic rays are quite well known, so estimates of the absorbed dose and specific ionization may be made on the basis of physical principles, even if there is some doubt about the biological effects (*9*).

A "solar-flare proton event" is usually characterized by a large optical solar flare (class 2 or greater), by type 4 solar radio noise, and by disturbances in the earth's ionosphere, such as polar-cap absorption of galactic radio waves. Occasionally, also, the flux of cosmic-ray neutrons in the lower atmosphere is enhanced. All the evidence points to the emission from the sun of a large, high-energy cloud of ionized protons which are intercepted by the earth. The incidence of solar-flare proton events seems to be correlated with sunspot number, but this has not been clearly demonstrated, since only a few solar cycles have been studied at all, and only the most recent (No. 19) has been studied in detail.

All the solar-flare proton events detectable during the most recent solar cycle were analyzed by Webber (*10*) in terms of the proton flux at the top of the atmosphere (and thus presumably in free space) from riometer data as well as balloon- and satellite-measured fluxes. Bailey (*11*) has inferred an energy spectrum and a time history "typical" of these events from the available riometer data at different latitudes. Webber and Freier have deduced the details of spectral variations with time during several such events (*3*).

The early data of Webber were rearranged by Chupp *et al.* to show an actual size-frequency distribution of solar-flare proton events (*12*). Since that work, newer analyses have been made by Webber and others of solar cycle 19

Table 1. Doses at five body points (unshielded and shielded*) from solar-flare protons for a typical exponential spectrum, with $P_0 = 100$ Mv, normalized to one proton of energy > 100 Mev per square centimeter.

Body point	Dose (rads proton^{-1} cm^{-2})				
	No shielding	Shielding, 1 g/cm^2	Shielding, 2 g/cm^2	Shielding, 4 g/cm^2	Shielding, 8 g/cm^2
Eye	3.0×10^{-5}	1.6×10^{-6}	8.3×10^{-7}	3.9×10^{-7}	1.5×10^{-7}
Sternum	3.0×10^{-7}	2.3×10^{-7}	1.8×10^{-7}	1.2×10^{-7}	6.7×10^{-8}
Chest skin	3.8×10^{-5}	1.8×10^{-6}	9.1×10^{-7}	4.0×10^{-7}	1.5×10^{-7}
Spleen	1.2×10^{-7}	1.0×10^{-7}	8.8×10^{-8}	6.6×10^{-8}	4.0×10^{-8}
Gut	6.2×10^{-8}	5.5×10^{-8}	4.8×10^{-8}	3.9×10^{-8}	2.7×10^{-8}

* Aluminum exterior shielding was used.

data, and the results have been published (*13*). Generally, the more recent inferred values for total proton flux integrated with respect to time are somewhat smaller than the values of the earlier report, and the energy spectra, rather than conforming to a power law, are thought to be exponential in form.

An important result of these published analyses of solar cycle 19 is shown in Fig. 1, in which the frequency of occurrence of a solar proton event having a flux greater than N is plotted against the total flux N of protons of energy greater than 100 million electron volts (Mev); in the calculation Webber and Freier's exponential spectrum is assumed (see *3*), and the flux-weighted average of the magnetic rigidity parameter P_0 for all the flares observed (100 megavolts) is used. Fifty-two events were observed during a 365-week period (February 1956 to October 1962), which included the solar cycle maximum. The average frequency of occurrence for this period is 0.14 solar-flare proton event per week. It should be noted, however, that the average frequency varied considerably from year to year, and that the number (eight) of "large" events is small enough to make us cautious about accepting these statistics as being definitive. In 1960 the average frequency of detectable events was 0.28 per week, while in 1959 and 1961 it was 0.11, and in 1962 it was 0.04, as the number of sun spots grew smaller. Hence, depending on time during the solar cycle, the maximum frequency of occurrence (the ordinate in Fig. 1) might vary from a value twice the value shown to a value less by an order of magnitude than the value shown. If it is assumed that these events or groups of events occur randomly in time, the average frequency for the period may be taken as the average probability per week of the occurrence of a flare event having flux at least equal to N (*14*).

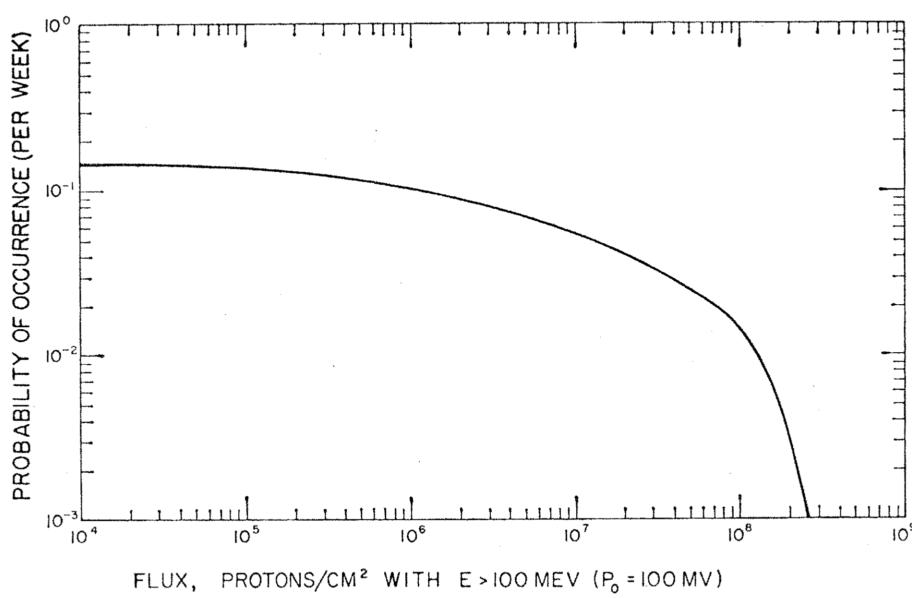

Fig. 1. Probability per week of the occurrence of a solar flare that produces an energetic proton flux near the earth, as a function of total time-integrated flux of protons with energy $E > 100$ Mev. Webber's data for the maximum of solar cycle 19 (*15*) and an exponential spectrum with $P_0 = 100$ Mv are assumed.

Although the energy spectrum of these particles varies from event to event, and during a single event, the exponential form $\exp(-P/P_0)$—where P is the magnetic rigidity in megavolts, with $P_0 = 100$ Mv—was taken as a typical spectrum. It should be noted that there is no apparent correlation of P_0 with flare size (as inferred from integrated flux), or with the position of the flare on the sun (*15*). Values for P_0 seem to be uniformly distributed between 45 and 150 Mv for all events of solar cycle 19. Thus our choice of 100 Mv for P_0, while it is an average value, leads simply to a representative energy spectrum that is convenient for illustrating our dose-computation concepts. This incident-energy distribution is used in the following discussion.

Shielding and Dose Calculation

Computational methods to determine what modification of proton spectra is effected by shielding materials have been described (*1*). Consideration has also been given to the secondary radiation generated in the shield by incident protons (*4*). Both the Monte Carlo method and less sophisticated methods have been used to evaluate the dose due to bremsstrahlung shields from incident electrons (*2*), as well as the doses from protons and the secondary radiations from these protons. In principle, the effectiveness of any shielding is calculable from known nuclear physical data on the interactions of energetic particles with matter. For example, yield cross sections for secondary nucleons as a function of incident proton energies and secondary particle energies have been studied extensively with cyclotrons and synchrotrons, and the experimental data from these studies, as well as theoretical data from Monte Carlo codes, are available for computing the effects of shielding (*16*).

For the typical observed energy spectra of space (*4*), it turns out that the secondary radiations from incident protons are important only for thick shields. Thus, the data of most importance to the calculation of shielding effectiveness against protons are the well-known range-energy relations that determine the penetration of the primary protons (*17*).

In computing the absorbed dose inside a space vehicle, one must take into account not only the angular distribution of the impinging radiation but also the angular distribution of shielding and structural materials around the point for which knowledge of the dose is desired. The simplest angular distribution of radiation is an isotropic flux; this is likely to be a sufficiently accurate description of the distribution for dose calculation if there is vehicle tumbling, even if the free-space flux is anisotropic. Therefore, we here assume isotropic incident flux. For calculating dose, the energy deposited in a specific organ or body point is the quantity of interest. Hence, the tissue of the body must be considered a part of the shielding material. Here the external configuration of the vehicle is assumed to be a spherical shell, but the computational procedures described are applicable to any vehicle structure.

For computing the dose at some point within a three-dimensional shielding configuration, the total solid angle around that point is divided, for analysis, into regions having essentially constant shielding. Each such region is then considered separately, and its contribution to the total dose is weighted according to the size of its fractional solid angle. Thus, a complex three-dimensional problem is converted to a set of one-dimensional problems.

A one-dimensional proton shielding-dose problem is rather easily calculated by computer and has been programmed for the IBM 7090 (*1, 4*). Briefly, the monodirectional incident proton spectrum, $P(E)\mathrm{d}E$, is modified by passage of the protons through the shield of thickness X according to the equations:

$$E' = EF(RF(E)-X), \qquad (1)$$

$$P'(E')\mathrm{d}E' = P(E)\mathrm{d}E\ (\mathrm{d}E'/\mathrm{d}E) \qquad (2)$$

and

$$\mathrm{d}E'/\mathrm{d}E = \frac{(\mathrm{d}R/\mathrm{d}E)_E}{(\mathrm{d}R/\mathrm{d}E)_{E'}} \qquad (3)$$

where $P'(E')$ is the energy spectrum of emergent protons, $RF(E)$ is the range-energy function (proton range as a function of energy), and $EF(R)$ is the inverse function for the shield material (*17*). These protons also produce neutrons, gamma rays, and secondary protons by nuclear interactions and scattering, and these secondary fluxes are attenuated by passage through the shield layers. The secondaries are generated according to the relation:

$$S(E_s)\mathrm{d}E_s = \int P(E_p, X) SMULT(E_p, E_s)\ \mathrm{d}E_s\ \sigma_s\ (E_p)\mathrm{d}E_p \qquad (4)$$

where S refers to any of the secondary components, E_s is secondary energy, $P(E_p, X)$ is the proton spectrum at depth X in the shield, $SMULT$ is a normalized distribution function describing the number of secondaries at each energy E_s produced by primaries of energy E_p, and $\sigma_s(E_p)$ is the cross section for yield of secondary component S by protons of energy E_p. (For more detail on such matters as angular distributions and secondary particle transmission through the shield, see *4*.)

The secondary-dose computer program is rather long, and secondary dose varies slowly with shield thicknesses greater than about 1 gram per square centimeter of aluminum (the initial transition region). The primary-dose code (derived from Eqs. 1–3 and from a dose calculation) is a rather short computer program, and the dose does depend strongly on shield thickness, especially for thin shields. Hence, as a means of saving computer time in seeking the total doses in a two-layer shielding problem, the computer is first used to calculate a matrix array of secondary doses for various thicknesses of the two layers of material. Then, for any specified thicknesses, a quick interpolation gives the secondary-dose value. The primary proton dose is calculated separately for each layer, and the total dose for the "one-dimensional" slab is then found by addition, after multiplication by appropriate relative biological effectiveness factors for the various components.

Finally, in a three-dimensional problem, to obtain the total dose at some body point, we add together the doses computed for the various regions of aluminum and tissue shielding, each weighted according to the region's fractional solid angle around the point in question.

Body-Point Dose

It is well known that a nonuniform dose in a large mammalian system elicits a response different from that elicited by a uniform whole-body dose; for example, K. L. Jackson has shown a significant increase in LD_{50} in rats with decrease in percentage of midline dose (*18*). It is also well known that certain organs and systems are more sensitive to radiation than others. In most of the quantitative studies performed to measure such radiosensitivity, LD_{50} has been the end point. When it is a question of the radiation hazard in space, it is desirable—indeed, necessary—that sublethal radiation effects be better known.

We previously reported (*4*) doses at 12 selected points in the body of a seated man (75-percentile body dimensions) (*19*) from certain power-law energy spectra of protons incident upon an aluminum spherical-shell shield around his body. The body-points selected for analysis included the sternum, spleen, spinal marrow, and femur in the hematopoietic system; the skin of chest and waist; the eye lens, which has been shown to be susceptible to cataract formation when linear energy transfer is high; and the central gut, representative of the intestinal wall, which, if damaged over wide areas, causes serious imbalance in body fluids. In each of these analyses the tissue of the body was considered to be a part of the shielding.

Five of these body-point doses have been recalculated, from more recently available data for the production of secondary radiation, and more recently determined energy spectra for proton flux in space. In every case our earlier contention that the secondary dose is a small fraction of the total (15 percent or less) is borne out. The previous results for total dose have generally been revised upward by about 10 percent as a result of the recalculation. The five body-point doses are given in Tables 1 and 2 for two reported proton spectra. Table 1 shows doses from the exponential solar-flare spectrum with $P_0 = 100$ Mv, and normalized to one proton per square centimeter over 100 Mev. Table 2 shows doses from the spectrum for the inner Van Allen belt, determined

Table 2. Doses at five body points (unshielded and shielded*) from trapped protons for the energy spectrum of Heckman and Armstrong (*5*), normalized to one proton of energy > 40 Mev per square centimeter.

Body point	Dose (rads proton^{-1} cm^{-2})				
	No shielding	Shielding, 1 g/cm^2	Shielding, 2 g/cm^2	Shielding, 4 g/cm^2	Shielding, 8 g/cm^2
Eye	1.6×10^{-7}	1.0×10^{-7}	8.7×10^{-8}	7.2×10^{-8}	5.1×10^{-8}
Sternum	6.2×10^{-8}	5.7×10^{-8}	5.3×10^{-8}	4.6×10^{-8}	3.5×10^{-8}
Chest skin	1.7×10^{-7}	9.8×10^{-8}	8.4×10^{-8}	6.8×10^{-8}	4.8×10^{-8}
Spleen	4.3×10^{-8}	4.0×10^{-8}	3.7×10^{-8}	3.3×10^{-8}	2.7×10^{-8}
Gut	3.4×10^{-8}	3.2×10^{-8}	3.0×10^{-8}	2.7×10^{-8}	2.2×10^{-8}

* Aluminum exterior shielding was used.

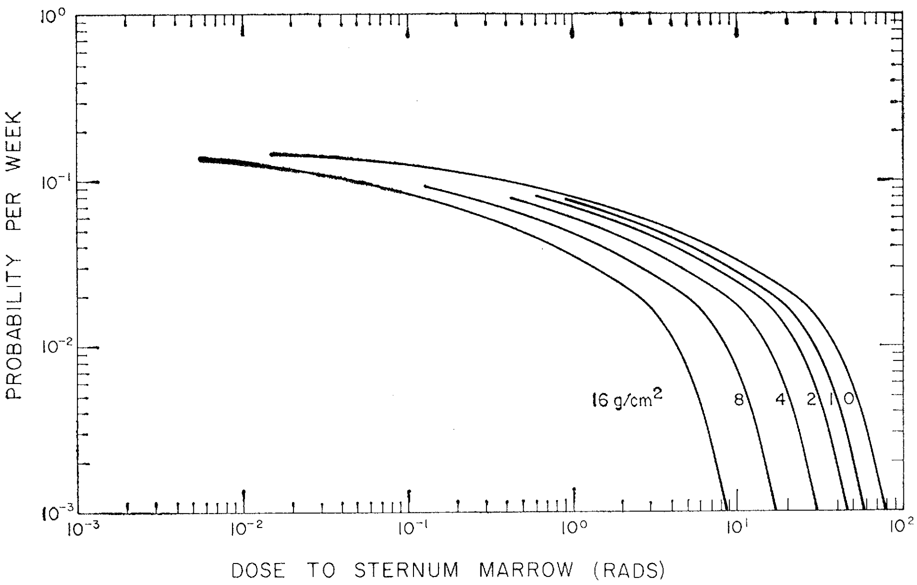

Fig. 2. Probability per week that the sternum will receive a specified dose (expressed in rads) from solar-flare protons under the conditions that existed during the maximum of solar cycle 19. It is assumed that the subject is seated within an aluminum spherical-shell shield; various thicknesses, ranging from 0 to 16 g/cm², are assumed for the shield.

experimentally by Heckman and Armstrong (*5*) and normalized to one proton per square centimeter over 40 Mev. (The dose computations take into account protons of all energies, but the spectra are normalized as indicated.)

The point-to-point variation in the dose absorbed by body organs of a seated human being in space demonstrates the need for this approach to the problem of radiation hazards. Tables 1 and 2 show variation by a factor of 2 between deep-body and surface-point doses when there is thick exterior shielding, and variation by a factor of 10 when shielding is thin. If, in an actual space journey, body-dose values in the range from 10 to 100 rads should be encountered, these variations by factors of 2 and 10 in dose distribution would be extremely important. The simple one-dimensional shielding model is inadequate for detailed evaluation of the radiobiological problems involved in space travel.

Evaluation of

Radiation Hazards in Space

For the moment, we will neglect the primary cosmic rays and the effect of fractionation or low dose rates in the trapped belts and consider only the solar-flare hazard. Figure 1 shows the probability of occurrence of a solar-flare proton event with total flux N (number, per square centimeter, of protons of energies greater than 100 Mev), as derived from Webber's data on solar cycle 19 (*15*). This curve may be translated into the probability per unit time that a specific body point shielded with a specified aluminum shell shield will receive a dose D (or less) from a solar-flare proton event. This is done by multiplying the values from the abscissa of Fig. 1 by the appropriate body-point dose from Table 1. Several such integral dose-probability curves are shown in Figs. 2 to 4, for, respectively, the sternum, gut, and eye lens. The doses at these three points represent, respectively, doses absorbed in blood-forming organs other than the sternum, in trunk, and in skin, generally to within a few percentage points. A striking feature of the data of 1 and 2 and of Figs. 2–4 is the wide variation in dose at these three representative body points. The eye, having little body shielding, is exposed to large doses unless there is appreciable external shielding by the vehicle. So is the skin of the lower leg or arm. The gut and the interior organs of the trunk generally have good body shielding. The sternum and the spinal column have a good chance of receiving doses of several tens of rads.

For example, consider the curves of Fig. 5, which show the dose rates for radiation from solar protons at three points in the body of a subject seated inside an aluminum shell (which provides shielding of 4 g/cm²) as a function of time during the period 10 to 20 July 1959. Three large solar-flare events occurred during this time. The proton intensities and P_0 values for these events have been given by Freier and Webber, and their values were used in calculating the data of Fig. 5. Both proton intensity and P_0 variations contribute to the fluctuations in dose rate. Changes in P_0 also affect the ratios of dose rate at the body surface to dose rate at deeper body points. The total doses for the period are computed to be 146 rads to the eye lens, 43.2 rads to the sternum, and 13.5 rads to the gut, for external shielding of the assumed thickness. This, again, points up the need to specify body locations in considering biologically significant doses from radiation in space.

Figures 2 to 4 are plots of the probability per week that a given solar-proton dose will be received at specific body points. These plots demonstrate the statistical nature of the hazard. We have as yet no way of knowing whether a solar-flare proton event will occur during some mission, or, if one does occur, what its size will be. However, the probability that an event of a given size, hence producing a given radiation dose, will occur may be estimated if these events or groups of events occur randomly in time.

On the other hand, the doses from trapped protons are determined by the trajectory and by shielding parameters for the mission and vehicle, as the doses from trapped electrons are. In a typical moon-launch trajectory the vehicle is exposed to a flux of 1.03×10^7 trapped protons, with energy greater than 40 Mev, per square centimeter. A flux of this strength, according to Table 2 for the Heckman-Armstrong spectrum, produces doses of 0.74 rad to the eye, 0.47 rad to the sternum, and 0.28 rad to the gut in a human being protected by external shielding with thickness of 4 g/cm². The same trajectory exposes occupants of the vehicle to bremsstrahlung of about 0.2 rad from trapped electrons.

Thus, for example, of a tolerance dose of, say, 25 rads to the eye, 1.7 rads will certainly be received from the trapped flux on launch and return, if the return trajectory is similar to the launch trajectory. This leaves 23.3 rads to be considered statistically. The probability, per week of space flight, of the eye's receiving a dose of 23.3 rads (in a vehicle which provides shielding of 4 g/cm²) is found, from Fig 4, to be 0.023. If this probability is not acceptable to mission planners, there are certain alternatives: increase the shielding to reduce the dose, perhaps with partial

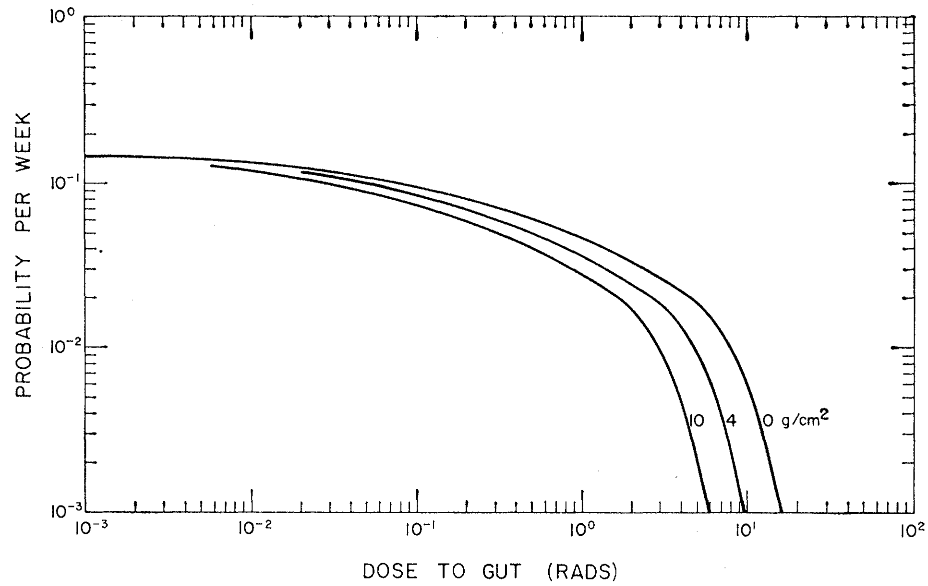

Fig. 3. Probability per week that the gut will receive a specified dose (expressed in rads) from solar-flare protons under the conditions that existed during the maximum of solar cycle 19. It is assumed that the subject is seated within an aluminum spherical-shell shield; various thicknesses, ranging from 0 to 10 g/cm², are assumed for the shield.

body shields such as goggles, or decide to allow a greater risk by raising the tolerance-dose levels, which are usually much lower than the dose levels that produce overt clinical symptoms. In Fig. 5 the dotted curve shows the dose rate to the eye if goggles which provide shielding of 4 g/cm² are worn during exposure. There is significant dose reduction, from 146 rads to 95 rads for the whole event. A change in the trajectory would reduce the dose from trapped protons somewhat, but would not significantly lower the probability of exceeding 25 rads.

In interpreting these curves, of course, one should remember that the probability that a solar-flare event will occur (Fig. 1) can be said to be known only to within a factor of 2. Some prediction schemes based on observation of the solar disk have been proposed, and if one of these methods proves valid it may be possible to avoid solar-flare events in planning space flights. Moreover, these curves apply to the maximum of the most recent solar sunspot cycle, and some statistical evidence exists which indicates that the next cycle will have fewer solar-flare events (*15*).

While the total dose from heavy particles ($A > 1$) in space appears to be small (about 1 millirad per day), these particles ionize heavily along their tracks and pose a possible biological hazard (*8*). It has been shown experimentally, by means of deuteron beams simulating heavy-particle tracks in tissue, that gross histopathological damage to brain and retina does not occur along the narrow tracks of alpha particles or of nuclei of the carbon, nitrogen, oxygen group (*20*). However, some cells are killed along these tracks of heavily ionized particles, and some sublethal effects must occur that are not observable by gross microscopic inspection. The alpha particles and heavier particles in the cosmic and solar rays undoubtedly kill cells when their velocity in tissue is sufficiently low, but the linear-energy-transfer value at which there is high cell lethality along their tracks is uncertain. If one chooses 85 kev/μ as the value for linear energy transfer at which every struck cell is killed, then the fraction of the cells killed in the body by the galactic cosmic rays in space is estimated to be 0.01 percent per day (*9*), and the single large solar flare of 16 July 1959 had enough alpha particles to kill 3 percent of the body cells in a man inside shielding of 4 g/cm². If 30 kev/μ is taken as the value for linear energy transfer certainly lethal to individual cells, then the fraction of body cells killed by cosmic rays in space is estimated to be 0.1 percent per day (*21*). These values may be compared to the average value of 0.003 percent per day for the fraction of body cells that die in the course of normal aging. From these estimates it may be seen that the heavy nuclei of cosmic rays can be an important hazard on a long space mission, but definitive radiological experiments on the effects of the death of body cells at these rates of linear energy transfer are yet to be made.

In an orbiting vehicle that is not continuously in the high flux region of the belts of trapped particles, the astronaut will receive fairly low doses, perhaps as little as a few rads per day to the hematopoietic system. In this case there will be some recovery during the exposure, allowing the astronaut to remain in orbit longer than would seem permissible on the basis of the tolerance

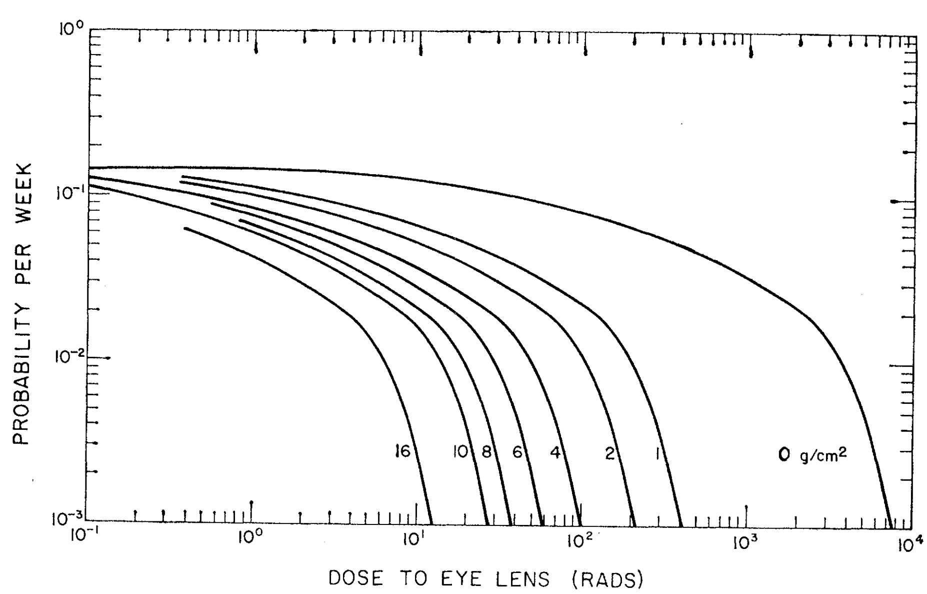

Fig. 4. Probability per week that the eye lens will receive a specified dose (expressed in rads) from solar-flare protons under the conditions that existed during the maximum of solar cycle 19. It is assumed that the subject is seated within an aluminum spherical-shell shield; various thicknesses, ranging from 0 to 16 g/cm², are assumed for the shield.

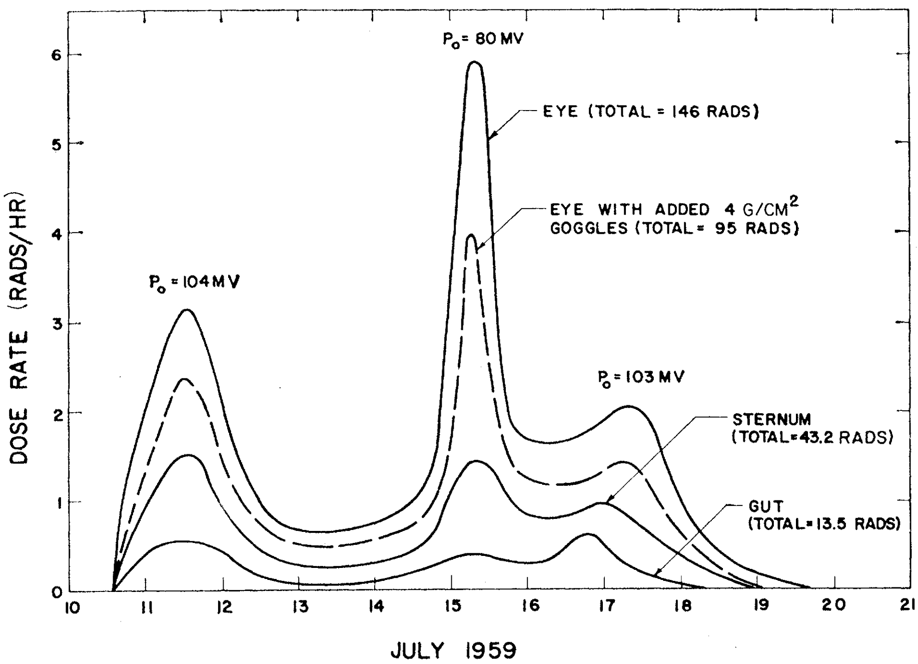

Fig. 5. Doses to the eye lens, sternum, and gut from solar-ray events like those that occurred between 10 and 17 July 1959. It is assumed that the subject is seated in the center of an aluminum spherical shell which provides shielding of 4 g/cm^2. The dashed curve shows the dose reduction effected by the use of glass goggles which give additional shielding of 4 g/cm^2. The total doses are calculated from the value for the integral flux and a flux-weighted average P_0 for each event.

dose alone. For example, a whole-body dose rate of 1 roentgen per day (delivered at a low linear energy transfer) leads to a total "equivalent residual dose" of 25 roentgens after 45 days (*22*). The degree to which specific organs recover from doses with high linear energy transfer is a subject for further study.

Planning a Space Mission

Briefly, the general procedures to be followed in planning to minimize radiation hazard in a manned space mission are as follows.

1) Determine as nearly as possible the doses that can be tolerated by radiosensitive body points.

2) Compute the body-point doses from trapped particles to be expected on a mission of the planned trajectory and with the planned vehicle structure.

3) For each body point, find the allowable dose from solar-flare proton emissions (the difference between the doses computed in procedures 1 and 2). Then, from integral dose-probability curves analogous to those of Figs. 2–4, find the probability that the allowed solar-proton dose to the organs will be exceeded.

If a specification is given of the desired reliability for a mission, one can find the body point for which the value for tolerance dose imposes the most severe shielding requirement, and perhaps provide special shielding. (For example, if the eye is critical, a special goggle shield might be designed which would reduce the dose by factors of 2 to 10, depending on the external structure.) Designing a mission vehicle and trajectory may require several iterations of this general process, since changes in vehicle design affect the computations of procedures 1 and 2. Furthermore, the radiation hazard is but one of several risks to be considered.

This approach to the problem of the radiation hazard in space is felt to be the most rational, for it takes account of (i) the specific radiosensitivities of individual organs, and (ii) the statistical nature of a large part of the absorbed dose. It allows the planners of a space mission to evaluate the hazard in terms of allowable dose to the most sensitive organ, on the basis of specific mission and vehicle parameters. Furthermore, it allows quantitative design trade-offs to be made between such factors as payload weight, trajectory, and the astronaut's short- or long-term ability to perform his job. In general, this approach points up the need for establishing reasonable tolerance-dose values for various organs. Much experimental work in radiobiology will be needed before there is universal agreement as to what values are reasonable; meanwhile, some intelligent guesses will have to be made. This approach also allows one to view the risks from radiation in perspective relative to the other hazards of space travel. It makes little sense to insist on 99.99-percent "radiation reliability" (or probability of 0.0001 that a tolerance will be exceeded) if the device for controlling the temperature of the astronaut's suit, for example, has only 99.0-percent reliability (1-percent chance of failure).

When there is quantitative understanding of the sublethal biological effects of cosmic rays with high linear energy transfer, these effects may be evaluated, along with the probable doses from trapped particles and particles from solar-flare events, to obtain a fairly complete picture of radiation hazards in space.

References and Notes

1. D. L. Dye and J. C. Noyes, *J. Astron. Soc.* **7**, 64 (1959); D. L. Dye and G. Butler, *ibid.*, **9**, 63 (1962).
2. "Proceedings of the Symposium on Protection Against Radiation Hazards in Space," *U.S. At. Energy Comm. Publ. TID-7652* (1962), pp. 409–793. For a detailed Monte Carlo analysis, see B. W. Mar, "The Calculation of Bremsstrahlung Radiation Penetrating a Space Vehicle," *Boeing Company Doc. D2-90411* (1963).
3. P. Freier and W. R. Webber, *Science* **142**, 1587 (1963).
4. D. L. Dye, in "Proceedings of the Symposium on Protection Against Radiation Hazards in Space," *U.S. At. Energy Comm. Publ. TID-7652* (1962), pp. 633–661.
5. H. H. Heckman and A. H. Armstrong, *J. Geophys. Res.* **67**, 1255 (1962); *ibid.*, bibliography.
6. C. E. McIlwain, *ibid.*, **66**, 3681 (1961).
7. F. C. Perry, "Proton fluxes along trajectories through the inner Van Allen belt," in "Proceedings of the Symposium on Protection Against Radiation Hazards in Space," *U.S. At. Energy Comm. Publ. TID-7652* (1962), pp. 725–738; also available as *Boeing Company Doc. D2-90306*.
8. H. J. Schaefer, in *Advances in Space Science*, F. L. Ordway, Ed. (Academic Press, New York, 1959), vol. 1, pp. 267–339.
9. W. R. Sheldon and D. L. Dye, paper presented at the 5th National Conference on Applied Meteorology, Atlantic City, March 1964; available as *Boeing Company Doc. D2-90529*.
10. W. R. Webber, "Time variations of low rigidity cosmic rays during the recent sunspot cycle," in *Progress in Elementary Particle and Cosmic Ray Physics* (Interscience, New York, 1962), pp. 77–243.
11. D. K. Bailey, *J. Geophys. Res.* **67**, 391 (1962).
12. E. L. Chupp, D. L. Dye, B. W. Mar, L. A. Oncley, R. W. Williams, *Boeing Company Doc. D2-11608* (1961).
13. P. S. Freier and W. R. Webber, "Exponential rigidity spectrum for solar flare cosmic rays," *J. Geophys. Res.* **68**, 1605 (1963).
14. In W. R. Webber, *Boeing Company Doc. D2-90469* (1963), a somewhat different method was used to treat the statistical problem of evaluating exposure probability for a specified mission duration, but it leads to the same numerical result as is here obtained for probability per week.
15. W. R. Webber, *Boeing Company Doc. D2-90469* (1963).
16. R. Wallace and C. Sondhaus, "Techniques used in shielding calculations for high energy

accelerators: Applications to space shielding," in "Proceedings of the Symposium on the Protection Against Radiation Hazards in Space," *U.S. At. Energy Comm. Publ. TID-7652* (1962), pp. 829–851; see also K. Strauch, "Measurements of secondary spectra from high-energy nuclear reactions," *ibid.*, pp. 409–432, and papers on Monte Carlo calculations by Oak Ridge National Laboratory workers at this same symposium.
17. M. Rich and R. Madey, *Univ. Calif. Radiation Lab. Rept. UCRL 2301* (1954).
18. K. L. Jackson, in "Proceedings of the Symposium on the Protection Against Radiation Hazards in Space," *U.S. At. Energy Comm. Publ. TID-7652* (1962), pp. 375–392.
19. D. L. Dye, *Health Phys.* **9**, 749 (1963). The "75-percentile man" analyzed is a composite body having each of its measurements equal to the 75-percentile value determined in an anthropometric study of Air Force personnel. Seventy-five percent of the subjects had smaller measurements.
20. H. J. Curtis, *Brookhaven Natl. Lab. Rept. BNL 6098* (1962).
21. W. R. Sheldon and S. B. Curtis, *Bull. Am. Phys. Soc.* **9**, 141 (1964).
22. "Exposure to Radiation in an Emergency," *Natl. Com. Radiation Protection and Measurement Rept. No. 29* (1962).

International Nutrition Programs

Improved food practices are essential to reasonable progress for a large part of the world's population.

C. G. King

Contrasts in food practices in various parts of the world are unbelievably great. They are fascinating to study and full of surprises, and they are often a dramatic index of health. Many individuals in all countries appear at least to be in good health, and probably are, but millions of others may be barely surviving in areas where food deficiencies are a major cause of sickness and death. One needs to consider large numbers of individuals to get a valid picture of the situation. Certainly the diets that are presented to most tourists are not indicative of what local populations eat routinely in rural, village, or slum areas.

Partly by choice, but chiefly from necessity, man has learned to survive on rations that differ greatly from the tenderloin steaks, frozen green peas, french fried potatoes, and strawberries with ice cream that one may have at any time of the year in large cities. Varied, attractive, and healthy diets are easily within the day-to-day reach of entire populations in technologically advanced countries. But in stark contrast, year-round diets are limited almost entirely to fish and potatoes on the island of Tristan da Cunha; to fish and seal in large areas of the arctic; to tree grubs, lizards, weeds, and kangaroos for primitive Australians; to rice with a few chick peas and some fresh vegetables for millions in India; and to corn, manioc (tapioca), beans, and plantain or coconuts in large areas of Africa and Latin America.

In areas such as the United States, Canada, and Western Europe, we no longer have an appreciable incidence of classical deficiency diseases such as rickets or scurvy, and when such diseases do occur, they are generally the result of gross individual neglect or stark ignorance. Nevertheless, although the life expectancy in these Western nations is twice that in many parts of the world, all countries share important problems related to nutrition, such as coronary heart disease, cerebral strokes, high blood pressure, overweight, diabetes, tooth decay, anemia, mineral imbalance, and special situations imposed by genetic abnormalities such as phenylketonuria and galactosemia, in which there is a failure to tolerate normal quantities of protein fragments and of milk sugar, respectively.

In nearly all areas where population density is high in relation to economic resources, there is a chronic or acute shortage of good-quality protein foods —a result of their relatively high cost and greater complexity and of the large amount of protein required in contrast to the small quantities of minerals and vitamins needed. Fortunately the high-quality protein foods such as meat, milk, poultry, fish, eggs, and, to a lesser extent, legumes such as beans and peas, are also good sources of minerals and vitamins. The animal protein foods have another great advantage in their flavor appeal.

Adequate medical and public recognition of the lack of sufficient good-quality protein as a major factor in high death rates, stunted growth, subnormal resistance to infections, and low nervous and physical vitality, has been slow to develop. The resultant penalty on health and economic progress has been and continues to be astounding.

A quick review of some facts will illustrate the tragedy that persists, as reported at the 1963 Conference on the Pre-School Child (*1*):

> The pre-school child, under five years, presents the major public health problem in developing countries today. Sickness rates are very high because these children are exposed to the usual diseases of childhood and also the parasitic infestations and infections of their environment. The mortality rates in the 1-to-4 years age group are sometimes forty times higher than the comparable rates among children of the same age in affluent countries. . . . It is estimated that 70 per cent of pre-school children in the developing regions of the world today are malnourished, particularly with respect to protein and calories.

Foundation for Progress

A healthy, vigorous populace is so basic to economic and social progress that this consideration of irreversible damage to pre-school children merits primary emphasis in every country (*2*). For those most handicapped educationally and technologically, the issue is particularly critical. Hence one of the most urgent services that technologically advanced countries can pro-

The author is associate director of the Institute of Nutrition Sciences at Columbia University, New York City, and chairman of the Committee on International Nutrition Programs, Food and Nutrition Board of the National Academy of Sciences-National Research Council, Washington, D.C.